5.6. Barrow, Alaska (11/10/99 – 11/27/00)

The 1999-2000 season at Barrow is defined as the time between the site visits 11/5/99 – 11/9/99 and 12/11/00 – 12/19/00. The season opening and closing calibrations were performed on 11/08/99 – 11/09/99 and 12/13/00, respectively. Volume 9 solar data comprises the period 11/10/99 – 11/27/00; the last day marks the start of the polar night. The system operated normally during this time but was affected by changes in responsivity of about 25%. These changes were compensated for by appropriately adjusting the calibration files. In certain periods, however, the calibration uncertainty is larger than usual. The observed drift has two causes: change of monochromator throughput and moisture condensing on the instrument's relay lens. A similar moisture problem has been observed in Barrow also during previous seasons, yet not to the same extent as during the Volume 9 period. A dehumidifier was installed in the roofbox during the site visit in December 2000 in response to the problem. About 95.5% of the scheduled data scans are part of the published dataset; less than 2% of all scans were lost because of technical problems.

During the site visit in November 1999, the PSP and TUVR instruments were removed, returned to Optronic Laboratories for recalibration, and installed again on 2/9/00. The new calibration factors were applied to the data in the Volume 9 season. These factors are presumably more accurate than the old factors that were established 1997. The TUVR calibration factor changed by 2.9%; the one for the PSP by 1.2%. The direction is such that irradiance values calculated with the new factor are higher for PSP and lower for TUVR. Note that PSP and TUVR are not heated. Since the instruments are only cleaned once per week snow may accumulate leading to a reduction in signal. In particular data from the first half of 2000 are affected.

5.6.1. Irradiance Calibration

The site irradiance standards for the 1999-2000 Barrow season were the lamps 200W009, M-762, and M-699. The lamp M-874 (calibration from Optronic Laboratories in September 1998) was used as the traveling standard during the season opening calibrations. As described in Sections 5.5.1 the lamp's irradiance changed after the site visit in Ushuaia in June 2000. The lamp was therefore replaced by the new traveling standard M-764, which was used during the season closing calibration. The history of M-764 is described in the introduction to Chapter 5 and in Section 5.5.1.

All three site standards 200W009, M-762, and M-699 were re-calibrated by Optronics Laboratories in September 1998, before they were used during the Barrow Volume 8 season. The same calibrations were also used in the Volume 9 season.

Figure 5.6.1 shows a comparison of all lamps at the beginning of the season (11/08/99 – 11/09/99). All site standards agree on the ±1.5% level with M-874. Figure 5.6.2 shows a similar comparison of all lamps for the end of the season (12/13/00), but now referenced to M-764. Lamps M-762 and M-699 are very consistent in the UV-A and visible, and agree in both spectral regions to within ±1.0% with M-764. In the UV-B, M-699 and M-764 deviate by 1.5 – 2%. Lamp 200W009 deviates systematically by 1.5 – 2.5% from the other lamps. This systematic offset was also observed during the season opening calibrations. A comparison with Volume 8 data suggests that the lamp drifted by 2% during Volume 8, but remained stable during Volume 9. Since a drift of 2% is still within typical uncertainties of lamp calibrations no adjustments were applied to correct for the drift.

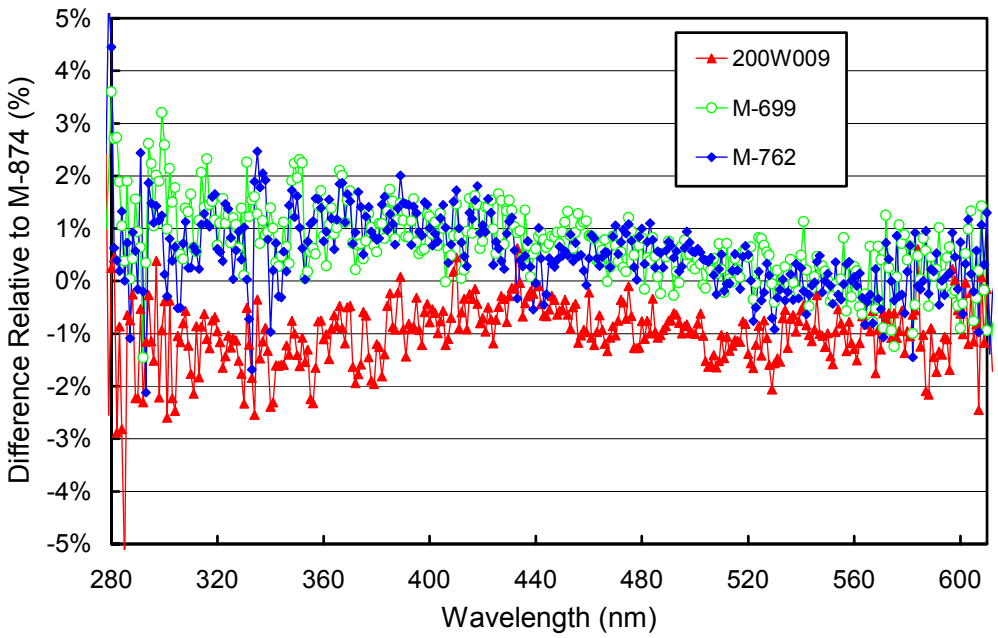

Figure 5.6.1. *Comparison of Barrow lamps 200W009, M-762, and M-699 with the BSI traveling standard M-874 at the beginning of the season.*

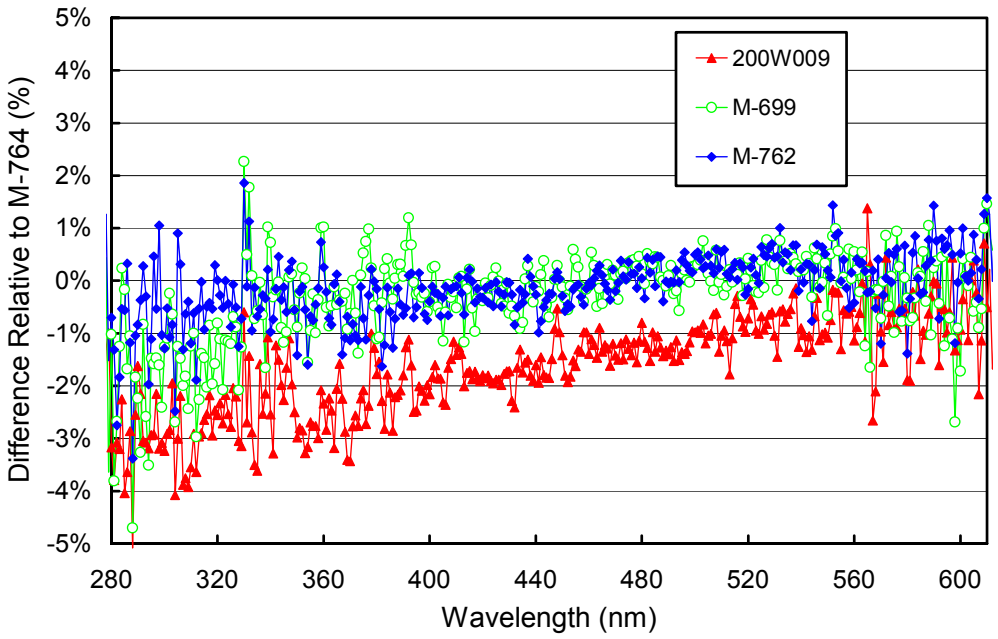

Figure 5.6.2. *Comparison of Barrow lamps 200W009, M-762, and M-699 with the BSI traveling standard M-874 at the end of the season.*

5.6.2. Instrument Stability

The stability of the spectroradiometer over time is primarily monitored with bi-weekly calibrations utilizing the site irradiance standards and daily response scans of the internal irradiance reference. The stability of the internal lamp is monitored with the TSI sensor, which is independent from possible monochromator and PMT drifts. Usually a new irradiance is assigned to the internal lamp when TSI measurements indicate that the lamp has drifted by more than 2%. This procedure could not be applied to Barrow Volume 9 data since the internal lamp was stable to within ±1.0% during the whole season, although absolute calibrations showed a drift of 25% during the same period. Part of the drift was due to moisture condensation on the relay lens located in the upper optical part of the instrument, which cannot be monitored with the internal lamp scans. The second reason is likely due to fluctuations in the monochromator throughput.

Figure 5.6.3 shows the changes in TSI readings and PMT currents at 300 and 400 nm, derived from the daily response scans. In addition, the PMT current measured at the 296.73 nm peak of the daily wavelength scans are shown. The TSI measurements indicate that the internal lamp was stable to within ±1% during the season. The PMT currents show a change of about 20% during the season. The drift observed during response scans is consistent with the drift in the peak signal of the 296.73 nm mercury line measurements. This suggests that the drift is caused by either the monochromator or the PMT. Further analysis indicates that the actual reason could be a change in the throughput of the monochromator. The throughput of a monochromator is in good approximation proportional to the square of its bandwidth. In order to determined whether a change in bandwidth caused the problem, the daily wavelength scans were evaluated, and the bandwidth determined. Figure 5.6.3 shows that the change of $(\text{bandwidth})^2$ has a similar pattern as the variation in PMT current, although to a smaller extent. This suggests that changes in bandwidth might indeed be the reason of the observed drifts. Fortunately solar data are only little affected by this instability since the change in monochromator throughput influences measurements of the internal lamp and through-the-collector solar measurements to approximately the same extent. The drifts are therefore compensated for by adjusting the system responsivity on a daily basis with the response scans.

Figure 5.6.3 also shows an abrupt change of 2.5% – 4% in PMT currents and $(\text{bandwidth})^2$ on 10/07/00. This change is due to a power failure, which exceeded the capacity of the uninterruptible power supply (UPS). During this time monochromator temperature fell temporarily from the target value of 33°C to 19°C and this might have permanently changed the monochromator bandwidth.

As mentioned above, moisture condensation on the relay lens was a second source of drifts in responsivity during the Barrow Volume 9 seasons. This drift was analyzed and corrected by analyzing the bi-weekly calibrations. This analysis suggested that 18 different irradiance spectra have to be assigned to the internal lamp to keep uncertainties caused by the drifts below a target value of ±2.0%. When changes between two consecutive calibrations were larger than 2%, the affected period was split in two or more parts. In each part, interpolated values were applied, which were calculated from the encompassing absolute scans. This is possible since the observed drift is a smooth function of time. The dashed lines in Figure 5.6.3 indicate the dates when a new calibration file was applied. Note that there were nine different files applied between 3/30/00 and 6/10/00. During this period, changes introduced by monochromator drifts were comparatively low.

Figure 5.6.4 shows the ratio of the irradiance assigned to the internal lamp in all 18 periods, referenced to Period “P2A” (01/01/00 to 02/17/00). Between Period “P3A” and Period “P11,” assigned lamp irradiance increases steadily with time.

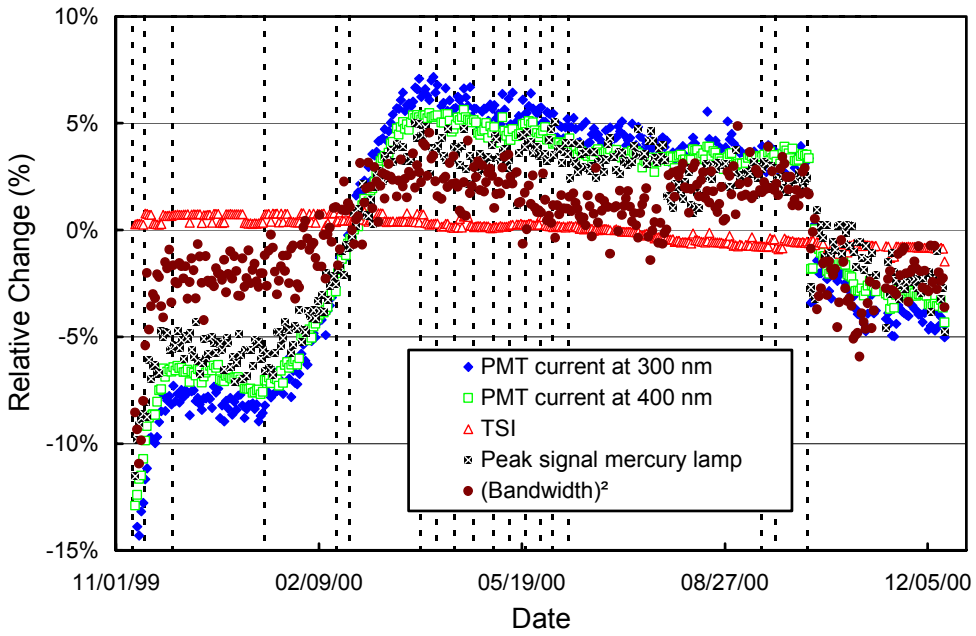

Figure 5.6.3. *Time-series of PMT current at 300 and 400 nm, and TSI signal, during measurements of the internal irradiance standard during the Barrow 1999-2000 season. White crosses show PMT current measured at the 296.73 nm peak of the daily wavelength scans; full circles are the square of the monochromator bandwidth as determined from the wavelength scans. All data sets are normalized to the average. Vertical dashed lines indicate dates when the calibration of the system was changed.*

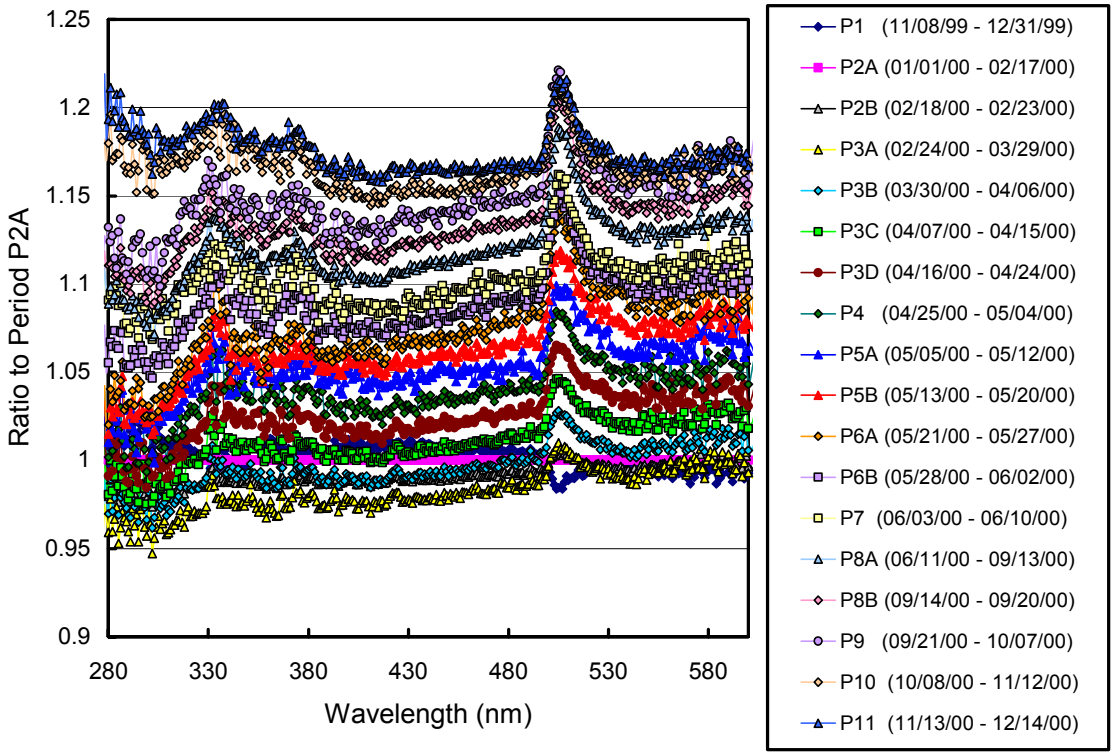

Figure 5.6.4. *Ratios of irradiance assigned to the internal reference lamp, referenced to Period P2A.*

Table 5.6.1 gives for each period the 1-σ Standard Uncertainty that is caused by the instrument drift. Note that this uncertainty is only a measure of the variability of calibrations in a given period. It is not the total calibration uncertainty, which would also include uncertainties in the calibration values of standard lamps. In periods when the system was stable the calibration file was derived by averaging the results of all absolute scans performed in this period (see Section 4.2.1.2 for details). These periods include periods P1, P2A, P3A, P8A, P10, and P11. The uncertainty for each of these periods is the ratio of standard deviation and average irradiance calculated from all calibration files performed in that period. These ratios are plotted in Figure 5.6.5. The 1-σ uncertainty is typically ±1% in the UV-B and ±0.6% in the visible. The uncertainty for periods when the calibration file was derived by interpolation was calculated from the uncertainty in the two calibration functions that form the starting-point of the interpolation, and the difference of those functions. The highest 1-σ uncertainty was found to be 2%. In spite of the observed drifts, uncertainties in published solar data remain in reasonable limits.

Table 5.6.1. 1-σ standard uncertainty of system calibration caused by responsivity drifts.

Period			Number of absolute scan	Standard uncertainty in %			Remarks
Label	Start	End		UV-B	UV-A	VIS	
P1	11/9/99	11/14/99	9	1.1	1.0	0.6	Standard calibration
P1	11/15/99	11/28/99	0	Unknown			Irrelevant because of low light levels
	11/29/99	1/12/00					Polar night
P2A	1/13/00	2/17/00	4	0.6	0.5	0.4	Standard calibration
P2B	2/18/00	2/23/00	0	1.4	1.0	0.9	Interpolation
P3A	2/24/00	3/29/00	3	0.7	0.6	0.7	Standard calibration
P3B	3/30/00	4/6/00		1.7	2.0	1.9	Interpolation
P3C	4/7/00	4/15/00		1.7	2.0	1.9	Interpolation
P3D	4/16/00	4/24/00		1.7	2.0	1.9	Interpolation
P4	4/25/00	5/4/00	1	1.1	0.9	0.6	Single scan
P5A	5/5/00	5/12/00	1	1.1	0.9	0.6	Single scan
P5B	5/13/00	5/20/00		1.6	1.4	1.1	Interpolation
P6A	5/21/00	5/27/00	1	1.1	0.9	0.6	Single scan
P6B	5/28/00	6/2/00		2.0	1.6	1.1	Interpolation
P7	6/3/00	6/10/00		1.1	0.9	0.6	Single scan
P8A	6/11/00	9/13/00	12	1.1	0.9	0.6	Standard calibration
P8B	9/14/00	9/20/00		1.7	1.5	1.2	Interpolation
P9	9/21/00	10/7/00	1	1.1	0.9	0.6	Single scan
P10	10/8/00	11/12/00	2	0.7	0.4	0.3	Standard calibration
P11	11/13/00	12/14/00	11	1.1	0.6	0.5	Standard calibration

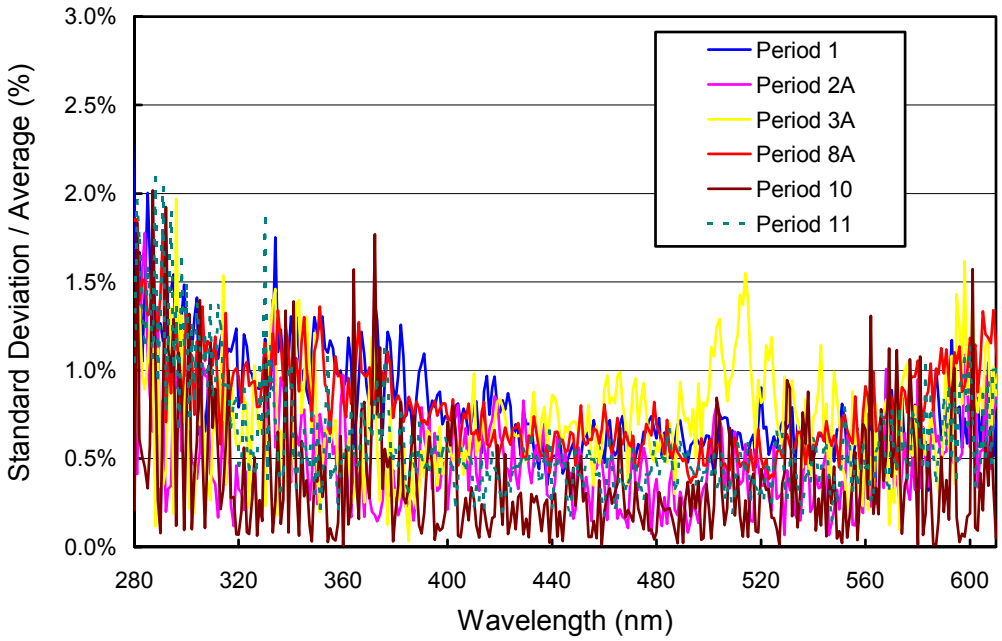

Figure 5.6.5 *Ratio of standard deviation and average calculated from the absolute calibration scans of selected periods.*

5.6.3. Wavelength Calibration

Wavelength stability of the system was monitored with the internal mercury lamp. Information from the daily wavelength scans was used to homogenize the data set by correcting day-to-day fluctuations in the wavelength offset. After this step, there may still be a deviation from the correct wavelength scale, but this bias should ideally be the same for all days. Figure 5.6.6 shows the differences in the wavelength offset of the 296.73 nm mercury line between two consecutive wavelength scans. In total, 393 scans were evaluated. For 93% of the days, the change in offset was smaller than ±0.025 nm. Only four scans showed a change larger than ±0.1 nm after manual wavelength adjustments.

After the data was corrected for day-to-day wavelength fluctuations, the wavelength-dependent bias between this homogenized data set and the correct wavelength scale was determined with the Fraunhofer-correlation method, as described in Section 4. The thick line in Figure 5.6.7 shows the resulting correction function that was applied to the Volume 9 Barrow data. The function depends upon wavelength, which is caused by non-linearities of the monochromator drive. In order to demonstrate the difference between the result of the Fraunhofer-correlation method and the method that was historically applied, Figure 5.6.7 also includes the correction function that was calculated with the "old" method, i.e., the function is based on internal wavelength scans only. The average difference between both approaches is approximately 0.14 nm. As explained in Section 4, this bias is caused by the different light paths for internal wavelength scans and solar measurements.

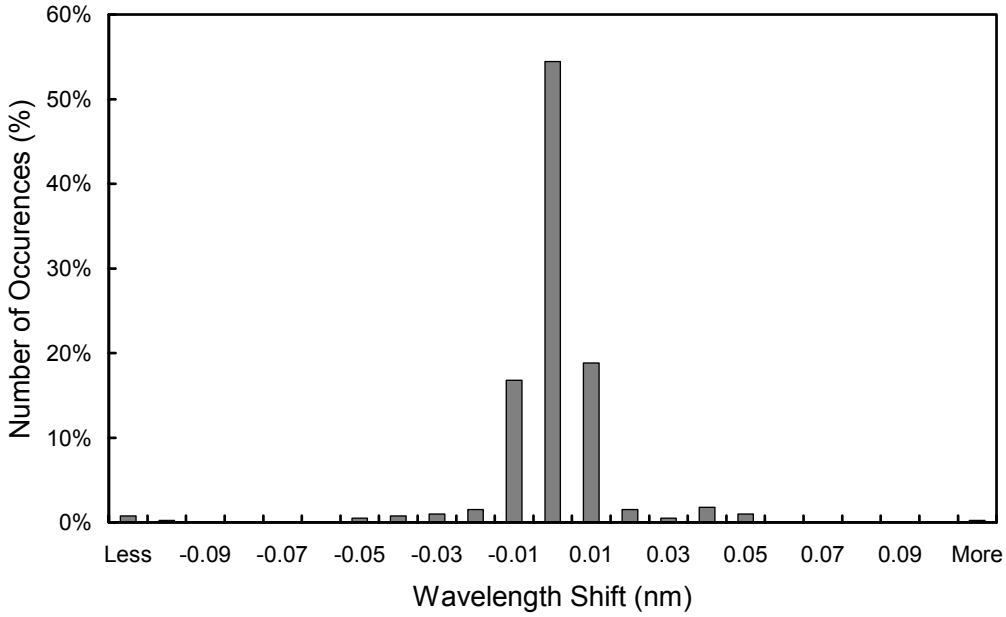

Figure 5.6.6. *Differences in the measured position of the 296.73 nm mercury line between consecutive wavelength scans. The x-labels give the center wavelength shift for each column. Thus the 0-nm histogram column covers the range -0.005 to +0.005 nm. "Less" means shifts smaller than –0.105 nm; "more" means shifts larger than 0.105 nm.*

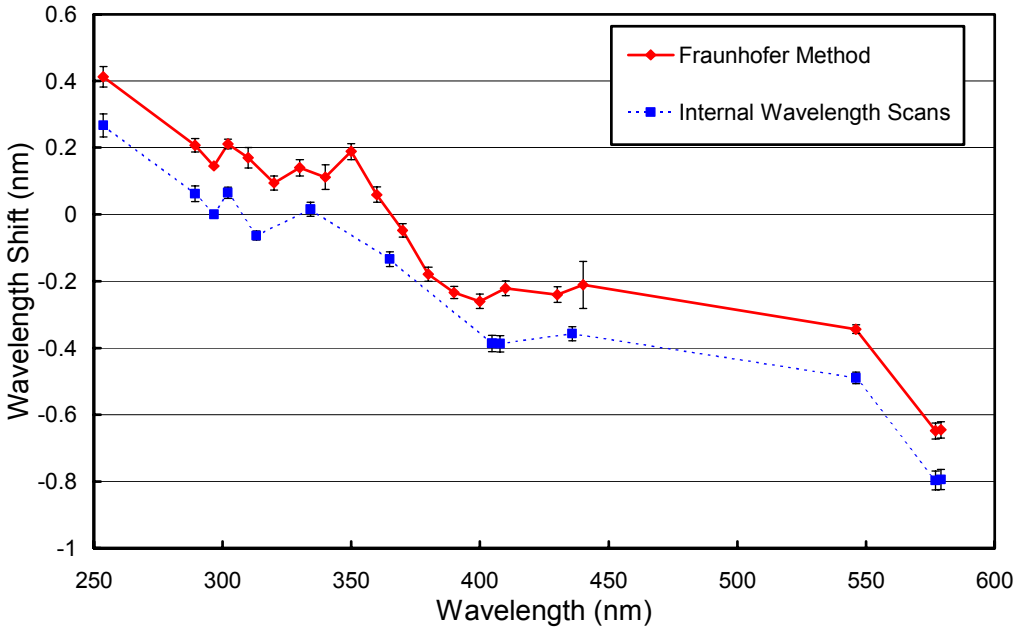

Figure 5.6.7. *Monochromator non-linearity for the Barrow 1999-2000 season. Solid line: correction function calculated with the Fraunhofer-correlation method, applied to correct the Barrow Volume 9 data. Thin broken line: correction function calculated with the method that was historically applied. The mean offset difference between both methods is 0.14 nm. The error bars show the 1σ standard deviation of the wavelength shifts for the season.*

After the data was wavelength corrected using the shift function described above, the wavelength accuracy was confirmed again with the Fraunhofer method. The results are shown in Figure 5.6.8 for four UV wavelengths, evaluated for all noontime scans measured during the season. The residual shifts are generally smaller than ±0.05 nm. The actual wavelength uncertainty may be larger due to wavelength fluctuations of about ±0.02 nm during the day, and possible systematic errors of the Fraunhofer-correlation method (see Section 4). There is also more scatter at 310 nm, in particular between the beginning of November and end of February because levels of solar irradiance at this wavelength are generally low at Barrow, which is problematic for the correlation algorithm. The enhanced scatter does not mean that the wavelength uncertainty is actually larger.

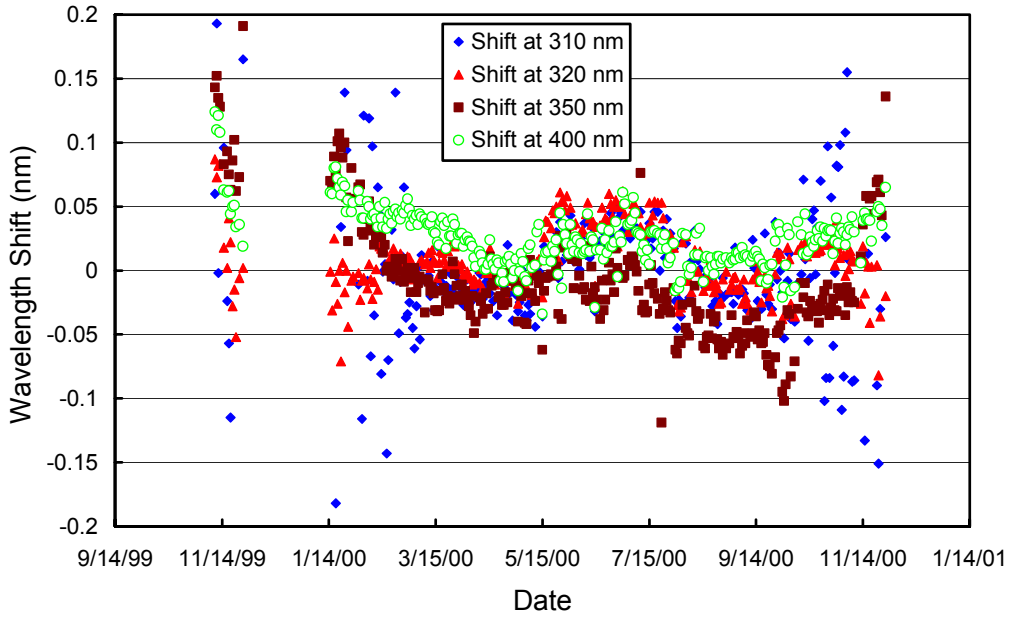

Figure 5.6.8. *Wavelength accuracy check of the final data at four wavelengths by means of Fraunhofer correlation. The noontime measurement has been evaluated for each day of the season when the sun was above the horizon.*

Although data from the external mercury scans do not have a direct influence on the data products, they are an important part of instrument characterization. Figure 5.6.9 illustrates the difference between internal and external mercury scans collected during both site visits. The wavelength scale of the figure is the same as applied during solar measurements. External scans have a bandwidth of about 1.07 nm FWHM, whereas the bandwidth of the internal scan was about 0.746 nm in 1999 and 0.762 nm in 2000. Although the somewhat higher bandwidth in 2000 is consistent with the change in (bandwidth)² shown in Figure 5.6.3, the difference is within the uncertainty in the bandwidth determination. The hypothesis that monochromator changes are partly responsible for the drifts observed can therefore not be confirmed unambiguously. Figure 5.6.9 also shows that season opening (November 1999) and season closing (December 2000) scans appear to be shifted by approximately 0.05. This is within the range of residual wavelength shifts after wavelength correction (see also Figure 5.6.8). Internal scans of both periods are shifted by about 0.18 nm to shorter wavelength with respect to their external counterparts. Since external scans have the same light path as solar measurements, they more realistically represent the monochromator bandpass relevant for solar scans.

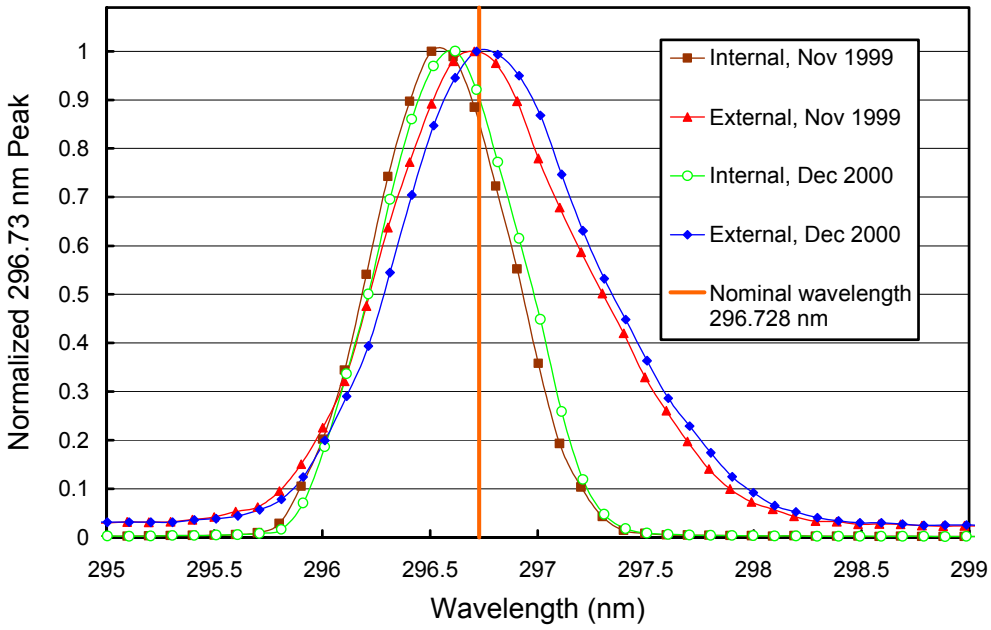

Figure 5.6.9. *The 296.73 mercury line as registered by the PMT from external and internal sources at the start and end of the season. The wavelength scale is the same as applied for solar measurements, i.e., it is based on a combination of internal scans and the Fraunhofer-correlation method. It is assumed that the wavelength registration of the monochromator did not shift between internal and external scans, which were close in time.*

5.6.4. Missing Data

A total of 19097 scans are part of the published Barrow Volume 9 dataset. These are 95.5% of all scans scheduled. Less than 2% of all scans were missed due to technical problems. Of all missing scans, 145, 187, and 182 were superseded by absolute, wavelength, and response scans, respectively. Due to power outages, which exceeded the capacity of the UPS, 37 scans were lost on 10/7/00 – 10/9/00. After the last scan on 11/9/00 the system stopped sampling until the computer was rebooted on 10/13/00, causing a loss of 58 scans. Similarly, no scans were recorded after the last scan on 3/8/00 until 04:15 GMT the following day, when normal operation was resumed without operator intervention. 17 scans were lost. Full hard drives led to losses of 34 data scans on 3/17/00, and 123 scans on 5/14/00 and 5/15/00. During computer clean up on 7/13/00, 8 scans were missed.